

Steven P. Christiano · Kenneth C. Fey

Silicone antifoam performance enhancement by nonionic surfactants in potato medium

Received: 13 March 2002 / Accepted: 26 August 2002
© Society for Industrial Microbiology 2003

Abstract The ability of a silicone antifoam to retard foaming in a liquor prepared from potatoes is enhanced by the addition of ethoxylated nonionic surfactants. The enhancement is non-linear for surfactant concentration, with all 12 surfactants tested possessing a concentration at which foam heights strongly diminish, referred to as the surfactant critical antifoaming concentration (SCAFC). SCAFCs vary between surfactants, with lower values indicating better mass efficiency of anti-foaming enhancement. SCAFCs decrease with degree of ethoxylation and decrease with the hydrophilic–lipophilic balance for ethoxylated nonionic surfactants. Surfactant addition produces a mixed water-surface layer containing surfactant and surface-active components in the potato medium. Surface tension reduction does not correlate well with antifoam performance enhancement. A model is proposed where surfactant adsorption promotes desorption of surface-active potato medium components from the water surface. At the SCAFC, desorption is not complete, yet the rate of bubble rupture is sufficiently enhanced to provide excellent foam control.

Keywords Foam control · Silicone · Antifoam · Nonionic surfactant · Potato liquor

Introduction

Foam formation is a general problem in industry and can be particularly difficult in protein solutions. In essence, two factors are necessary for foam to form: (1) a process that disperses a gas into a liquid to form bubbles and (2) stabilization of bubbles through adsorption of a surface-active material at the water surface. Foam

formed during fermentation is stabilized by components present in the growth medium and by fermentation products, such as extracellular proteins or other biological molecules [19, 24]. For example, a complex blend of extracellular proteins, lipophilic compounds, and α -keto acids were isolated from foam arising during a fungal fermentation [17]. Carbohydrates can also contribute to the stabilization of foam [25].

Adsorption of protein is driven by the reduction in surface tension that occurs when hydrophobic amino acid side-chains are exposed at the water surface [3, 16]. Protein adsorption stabilizes foam by providing a kinetic barrier to the rupture of bubble films and by retarding the rate of solution drainage from the foam. At protein adsorption levels above about 1 mg/m², a steep decrease in surface tension and an increase in surface shear modulus is observed. At higher adsorption levels, these properties level off [1]. At 1–3 mg protein/m², interfacially adsorbed protein forms a viscoelastic gel-like layer composed of surface adsorbed segments and loops extending about 5 nm into the solution [5, 7, 18].

The use of antifoam agents in fermentation is quite widely practiced [9]. Antifoams are theorized to act through four key mechanistic steps: (1) entering, (2) bridging, (3) dewetting, and (4) rupture [6]. Figure 1 schematically illustrates these steps. The silicone antifoam droplet becomes trapped within a thinning water film (Fig. 1a), such as a bubble film [4] or the Plateau border that forms between three bubbles [28, 29]. In either location, as solution drains from the foam, the antifoam droplet is pushed against the water surface, causing it to “enter” the water surface and achieve contact with air (Fig. 1b). Further drainage and thinning promotes a second entering step, causing the antifoam droplet to “bridge” the width of the film (Fig. 1c). Because the oil is hydrophobic, the water film adopts a high contact angle (Fig. 1d) and, with further thinning, the bubble film disengages from the antifoam droplet, rupturing the film (Fig. 1e) which withdraws rapidly. The antifoam droplet is thought to withdraw from one side of the bubble film [30]. Although not explicitly

S.P. Christiano (✉) · K.C. Fey
Dow Corning Corporation,
P.O. Box 994,
Midland MI 48686, USA
E-mail: s.christiano@dowcorning.com

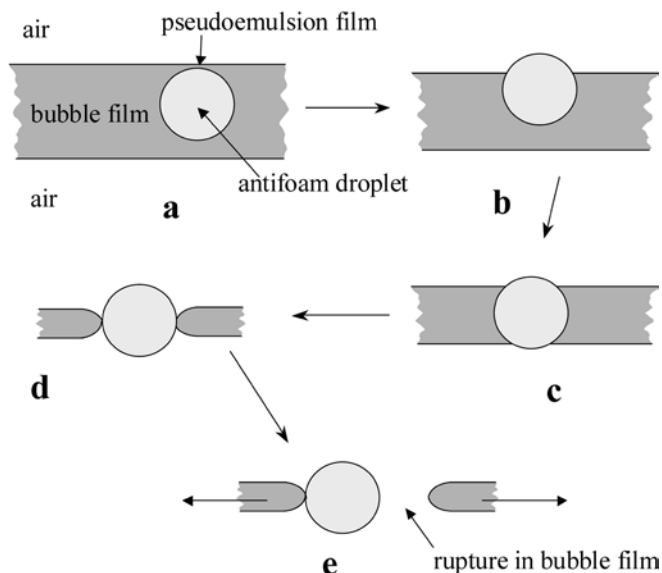


Fig. 1a–e Schematic antifoam mechanism. An antifoam droplet within a thinning water film approaches the water surface, forming a pseudoemulsion film (a) and enters the water surface (b). Further thinning promotes a second entering step and causes antifoam droplet bridging (c). The water film de-wets the antifoam droplet (d). Further bubble film thinning leads to rupture of the bubble film (e)

shown in Fig. 1, the antifoam fluid may spread across the surface of the water after it has entered [10].

The thermodynamics of the entering step are evaluated using the entering coefficient, $E = \gamma_w + \gamma_{o/w} - \gamma_o$, where γ_w and γ_o are the surface tensions of the aqueous solution and antifoaming oil, respectively, and $\gamma_{o/w}$ is the interfacial tension between the water and the oil droplet [21]. A positive value for E signifies a thermodynamically favorable process. E values for silicone antifoam in protein solutions will typically be positive.

It is theorized that the kinetics of entering determines whether foam control is achieved. The rate of bubble rupture must equal or surpass the rate of bubble formation to avoid foam buildup. The rate of entering, thought by many to be the rate-determining step, is determined by the stability of the thin water film, known as the pseudoemulsion film, formed as the antifoam particle approaches the water surface (Fig. 1a) [13]. The presence of a viscoelastic protein surface layer is expected to be a barrier to drainage and the collapse of the pseudoemulsion film and is therefore expected to diminish the antifoam-derived bubble rupture rates.

However, by modifying the surface-adsorbed protein layer, it may be possible to impact antifoam entering rates. Surfactants can have a profound effect on the properties of interfacially adsorbed protein [22], such as the surface shear viscosity [2]. Recently, atomic force microscopy (AFM) provided a clear demonstration that a significant reorganization of the surface layer occurs when surfactant is added to a protein solution. Surfactant-rich domains form between segregated

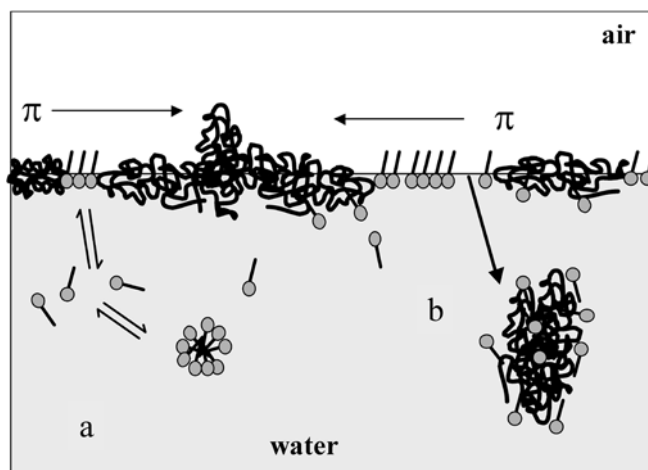


Fig. 2 Summary of surfactant surface pressure and desorption mechanisms [14]. Surfactant molecules in solution adsorb between surface-adsorbed protein molecules (*two-way arrows, a*). With increased surfactant concentration, adsorption applies a surface pressure, π , to the protein molecules and causes a reorganization and protein segregation. Surfactant adsorption onto the protein's hydrophobic regions aids in protein desorption (*thick arrow, b*)

tendrils of surface-adsorbed protein [14]. Figure 2 summarizes the phenomena expected when surfactant (in solution and possibly as micelles) adsorbs at the water surface to form a mixed surface layer with protein. As surfactant concentration increases, the surfactant exerts a lateral force, a surface pressure, π , on the protein. Surface pressure is the change in surface tension as surfactant adsorbs at the water surface. Thus, $\pi = \gamma_{\text{protein}} - \gamma_{(\text{protein} + \text{surfactant})}$, where γ_{protein} is the surface tension of the protein solution and $\gamma_{(\text{protein} + \text{surfactant})}$ is the surface tension of the mixed protein and surfactant surface layer. With increasing surface pressure, the protein remains surface-adsorbed but segregates into thickened domains that project upward from the water surface. This form of protein redistribution is referred to as the surface-pressure model (Fig. 2a). At higher surfactant concentrations, protein desorption from the surface is observed [14]. Surfactant adsorbs to the protein and promotes desorption back into solution (Fig. 2b).

Many commercial antifoams are complex mixtures of oils and surfactants. A better understanding of how these systems work is needed. Improved antifoam efficiency will contribute to fermentation productivity and will ease downstream processing. Improved longevity of antifoam may reduce the need for repeated dosing of antifoam often needed during the later stages of fermentation [11].

Methods and materials

Potato liquor

Peeled, sliced Idaho russet potatoes (900 g) and 360 g of deionized water were mixed for 60 s in a blender to form a slurry of

potato bits in water. The slurry was strained through double layers of cheesecloth, resulting in a white suspension. The suspension was allowed to settle for 90 min and was then decanted to provide 600 g of tan or reddish-brown turbid solution. This liquor was not controlled nor analyzed for protein or starch content but was used as prepared. Unadulterated liquor samples showed a high level of reproducibility in their foaminess. A significant variability in foaminess in the presence of antifoam was noted. Nonvolatile (105 °C) solids content for the potato liquor was 9.1 ± 0.7 g/l.

Bubble film optical microscopy

A bubble film was supported across a 5×2 mm oval perforation on a stainless steel plate (0.75 mm thick). The plate was attached to a glass slide with a gap centered below the perforation. The film was formed by drawing a foaming medium across the perforation and was then thinned by wicking the solution from the perimeter into a paper wipe. The film was viewed by transmitted light using an Axioskop microscope (Carl Zeiss), fitted with differential interference contrast optics. Images (640×480 pixels) were captured using a charge-coupled device (CCD) camera (Hamamatsu XC-77; C2400 controller) interfaced with a PC, using Flashpoint FPG software (Integral Technologies). Four or five potato liquor bubble films were observed using this technique.

Laser interferometry

Using the method of Snow et al. [23], bubble films were drawn on stainless steel frames with a rectangular 10×20 mm cutout. Films were formed within a capped rectangular cuvette as the frames were withdrawn from the foaming solution by a computer-controlled stepper motor (Arrick Robotics MD-2, interfaced with a PC) at a rate of 25 mm/s. The draining film was monitored by interferometry, using a HeNe laser (632.8 nm) reflected off the film at an angle of approximately 30 degrees. The changing interference pattern was recorded using a black and white CCD camera (Pulnix TM-745E, 765×493 pixels, with a Pulnix CCU-84 camera controller) and a video recorder (Sony Hi-8 EVO-9500A). Four or five films of surfactant-based detergent and potato liquor bubble films were observed.

Surface tension

The du Nouy ring method was employed, using a tensiometer (Kruss K6). Samples were allowed to equilibrate for 30 min prior to the measurement of surface tension. Surface pressure, π , was calculated as the difference between the surface tension of the unadulterated potato liquor (average of 38 mN/m) and potato-liquor with surfactant added. Values cited are the average of five measurements at 22 °C.

Sparging cylinder method

Samples (100 g) of potato liquor were prepared. Antifoam and surfactant ingredients (± 0.01 g) were dosed into the samples and were mixed by slow inversions. The sparging cylinder was a 22 °C jacketed glass cylinder, 5 cm in diameter and approximately 85 cm high. A vertical gas sparging tube fitted with a sintered glass frit (type C) was mounted approximately 2 cm below the surface of the solution. The nitrogen gas-flow rate (295 ml/min) was controlled using a gas-flow controller. This rate was held constant for all experiments. Data from two experiments run on different lots of potato liquor were averaged. The foam height above the solution was measured in centimeters, or was expressed as a relative reduction in foam height: $\Delta F_{rel} = (F_0 - F)/F_0$, where F_0 is the 8-min foam height with antifoam present and F is the 8-min foam height with antifoam and surfactant added.

Commercial antifoam emulsion and surfactants

Dow Corning 1520 silicone antifoam was used as received. This material is a silicone-in-water emulsion reported to contain 20 wt% silicone actives.

Surfactants were used as received from the manufacturers. Tween 65 is a polyoxyethylene 20 sorbitan tristearate and Tween 85 is a polyoxyethylene 20 sorbitan trioleate (Uniqema). Tergitol 15-S-3, Tergitol 15-S-5, Tergitol 15-S-7, and Tergitol 15-S-9 (Dow Chemical Company) are ethoxylated C_{11-15} secondary alcohols, with an average degree of ethoxylation indicated by the final digit of the name. Triton X-100 is octylphenol polyoxyethylene 10 (Dow). Aldo MS is glycerol monostearate (Lonza). Sodium oleate was received from Aldrich. Neodol 25-7 and Neodol 25-9 (Shell Chemical Company) are C_{12-15} linear alcohol with an average of seven and nine ethoxylates per molecule, respectively. Hydrophilic-lipophilic balance (HLB) values for the surfactants are as listed in supplier information or as reported [15].

Results

A liquor produced by slicing potatoes was chosen as a foaming medium relevant to food processing and fermentation, in that it contains a complex mixture of starches and proteins. Microburet analysis of potato liquors show that a variety of proteins, possibly greater than 20 distinct proteins, are present [27]. That complexity may contribute to foam formation or stabilization in a way that is missing with media based on a single purified protein.

The potato liquor readily foams with shaking or sparging, producing highly stable, visually opaque foam containing bubbles 2–5 mm in diameter. There is sufficient fluid holdup within the foam, even after hours of draining time, that the foam retains the reddish or tan color of the underlying potato liquor. Potato liquor foam was observed to have noticeably thicker bubble films and Plateau borders, compared with foams obtained with surfactant solutions.

The microscopic appearance of potato liquor bubble films was explored using a novel optical microscopy method. Figure 3 contains a micrograph of a potato liquor bubble film. The thickened perimeter around the bubble film is the bright region and, consequently, the film has a gradation of increasing thickness toward the lower right. A large number of visible particles are entrapped in the film, causing protrusions into the bubble film surface. These particles vary in their size, appearance, and chemical makeup. The more compact or rounded particles contain starch (β -amylose), as evidenced by the blue color formed upon iodine treatment. Other solids present have a flexible threadlike appearance and do not take on coloration with iodine. Particles with an average size of 5–10 μ m are visible in Fig. 3 and are immobile in the film. Finer particulates (not visible in the figure) float freely within the film. Surfactant bubble films observed using this technique are quite featureless and are devoid of entrapped particles.

Laser interferometry was used to directly observe the dynamic thinning of bubble films. Fig. 4a contains an image of a bubble film drawn from a solution of a liquid

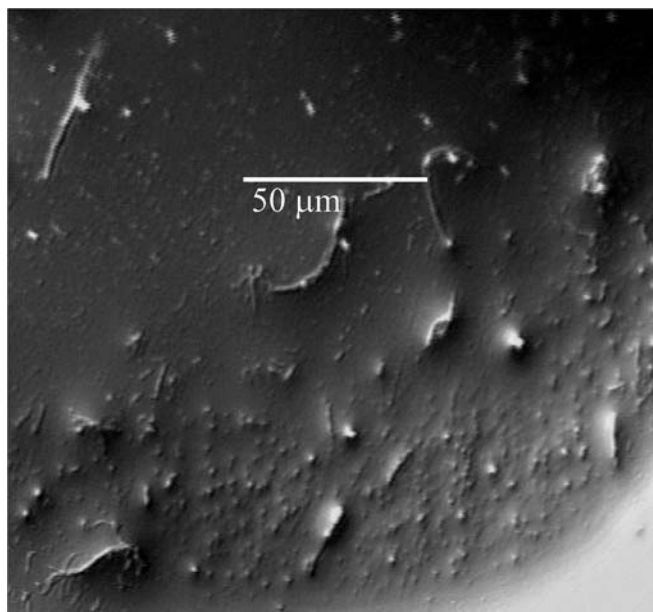


Fig. 3 Optical micrograph of a potato liquor bubble film at 200 \times magnification, showing particles trapped within the bubble film. The film is suspended across a hole in a stainless steel plate

detergent after it drained for about 15 s. The horizontal dark lines arise from destructive interference when laser light is reflected from the front and rear surfaces of the bubble film. The orderly horizontal alignment of the interference lines indicates a smoothly increasing bubble film thickness from top to bottom. With time, fluid drains from the film, reducing the gradient of thickness change down the film and reducing the number of interference lines. These films thinned until spontaneous rupture occurred, typically within about 4 min after bubble film formation.

Figure 4b shows an interferograph of a potato liquor bubble film after 1 min of drainage. The image differs from the soap bubble film in that the interference lines follow a far more complicated pattern. The interference lines have upward deviations, indicating localized increases in film thickness. There are closed circular interference lines within some of the undulations, interpreted as protrusions into the film surface. The increases in film thickness probably coincide with the presence of particles entrapped in the film.

These particles had a profound impact on drainage of fluid from potato liquor bubble films. Over the course of about 10 min, the interference lines became increasingly undulatory and slowed in their movement down the film, indicating very slow or ceased film drainage. The potato liquor bubble films remained stable in this semi-drained state for tens of minutes to hours.

The ability of a commercial silicone antifoam to impact the rate of foam formation in potato liquor was assessed using a sparging cylinder. Figure 5 illustrates typical foam growth behavior. The unadulterated potato liquor produced a growth of foam height linear with sparging time. Addition of the commercial antifoam

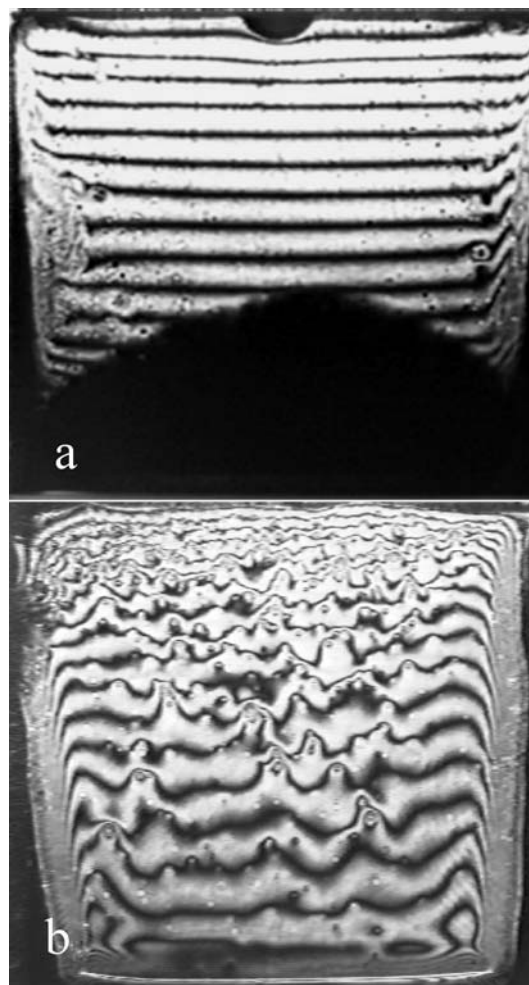


Fig. 4a, b Laser interferographs of bubble films formed on metal frames partly withdrawn from solution. **a** Surfactant film, showing horizontal interference lines indicative of orderly thickness progression. **b** A potato liquor bubble film showing highly convoluted interference lines, attributed to particles trapped within the film

produced a foam height that was non-linear with sparging time, initially showing a high rate of foam rupture and low growth of foam height. After about 5 min of sparging, the rate of bubble-rupture decreased and, after about 8 min, an unabated rate of foam generation was acquired, with a rate of growth essentially equaling that of the unadulterated sample. Addition of Tween 65 surfactant at 30 ppm and 240 ppm decreased the foam height at short sparging times to the minimum level measured by the technique. At longer sparging times, progressively lower foam heights were measured with increasing surfactant concentration. The values measured after 8 min of sparging were judged to be generally indicative of the trends observed and showed that the combination of antifoam and Tween 65 surfactant offered a significantly enhanced performance over the antifoam by itself.

Antifoam performance enhancement was investigated using the surfactants listed in Table 1. As was illustrated

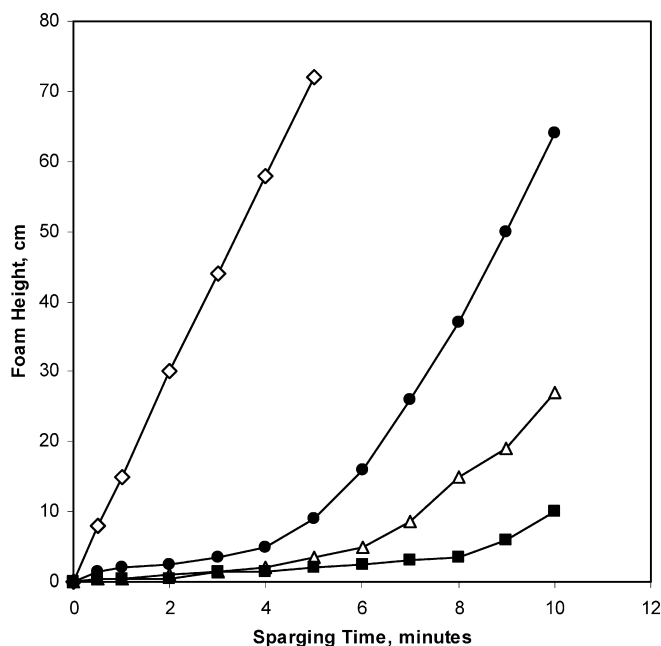


Fig. 5 Foam height in an actively sparged (22 °C) column, with undiluted potato liquor (*white diamonds*), with 50 ppm of silicone antifoam added (*black circles*), and potato liquor with both antifoam and Tween 65 surfactant added at 30 ppm (*white triangles*) and at 240 ppm (*black squares*)

for Tween 65, the surfactant enhancement depended on surfactant concentration. Figure 6 illustrates a typical result as concentration of Tergitol 15-S-7 was varied. The sparging foam height decreased when the 15-S-7 surfactant concentration was varied from 0 ppm to 250 ppm.

Qualitatively, the same response was observed with all the surfactants tested and it can be generalized to contain three regions. At low surfactant concentrations, there is little decrease or even an increase in foam height, relative to the silicone antifoam by itself. In the second surfactant concentration range, there is a strong reduction in foam height. In the third surfactant concentration range, the foam height reaches a minimum and changes little with surfactant concentration. For some

surfactants, for example the anionic surfactant sodium oleate, the height of the foam at its minimum plateau (third concentration range) is still quite high (17 cm), suggesting there is a limitation as to its effectiveness.

In the second concentration range, the sparging foam height was observed to fall quite precipitously at a concentration particular to each surfactant. The concentration at which the foam height falls to the minimum plateau is referred to as the surfactant critical antifoaming concentration (SCAFC). This value is useful for comparing the efficiency of different surfactants for enhanced antifoaming. Some surfactants approached the low foam height plateau asymptotically, in which case the intersection of lines extrapolated from linear portions of the foam height vs surfactant concentration curve were used as the surfactant's SCAFC.

The relationship between surface tension and SCAFC was explored by measuring the surface tension of the potato liquor with surfactant added, but prior to addition of the silicone antifoam emulsion. Figure 7 illustrates the impact of Tergitol 15-S-9 on antifoam efficacy. The foam height decreased with surfactant concentration, giving a SCAFC of around 64 ppm. The surface tension of the potato liquor was initially about 38 mN/m and decreased with surfactant concentration. However, the surface tension did not decrease smoothly, as expected in pure water, but showed a clear break-point or inflection-point, indicating a change in slope. As shown in Fig. 7, the break-point occurred at approximately the same surfactant concentration as the SCAFC. A surface tension inflection-point was observed with all the samples tested, except sodium oleate.

Table 1 includes the SCAFC measured for each surfactant, the surface tensions at the SCAFC, and the surfactant concentration giving a 50% reduction in the sparging foam height. The surface pressure at the SCAFC and the surfactant concentration at which an inflection or slope change in the surface tension curve was observed are also included in Table 1. Surfactants for which the inflection-point coincides with the SCAFC are highlighted. HLB values reported for the surfactants

Table 1 Surfactant critical antifoaming concentration (SCAFC), surface tension at the SCAFC, surface pressure at the surfactant SCAFC, surfactant concentration at which an inflection or slope-change is noted, and reported hydrophilic-lipophilic balance (HLB) values

Surfactant	SCAFC (ppm)	Surface tension at SCAFC (mN/m)	Surface pressure at SCAFC (mN/m)	Surface tension inflection concentration (ppm)	Surfactant HLB
Glycerol monooleate	110	35	4	300	3.0
Sodium oleate	55	38	1	240	21.0
Neodol 25-7	67	35	4	133	12.3
Neodol 25-9	65	34	5	65	13.1
Tergitol 15-S-3	230	32	7	230	8.3
Tergitol 15-S-5	82	34	5	240	10.6
Tergitol 15-S-7	60	35	4	70	12.4
Tergitol 15-S-9	40	34	5	64	13.3
Triton X-100	45	33	6	45	13.5
Tween 65	120	38	1	250	10.0
Tween 85	35	38	1	35	11.0

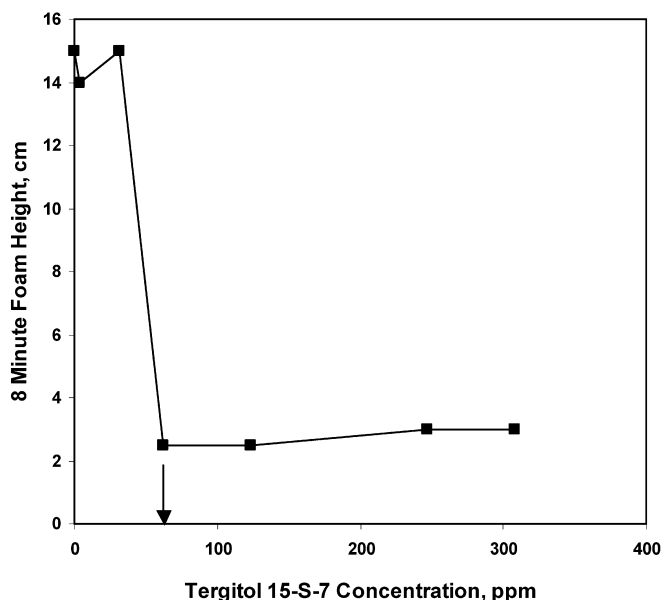


Fig. 6 Sparge test (8-min) foam heights of potato liquor containing 50 ppm of silicone antifoam emulsion and varying in Tergitol 15-S-7 surfactant concentration. *Arrow* indicates the surfactant critical antifoaming concentration (SCAFC)

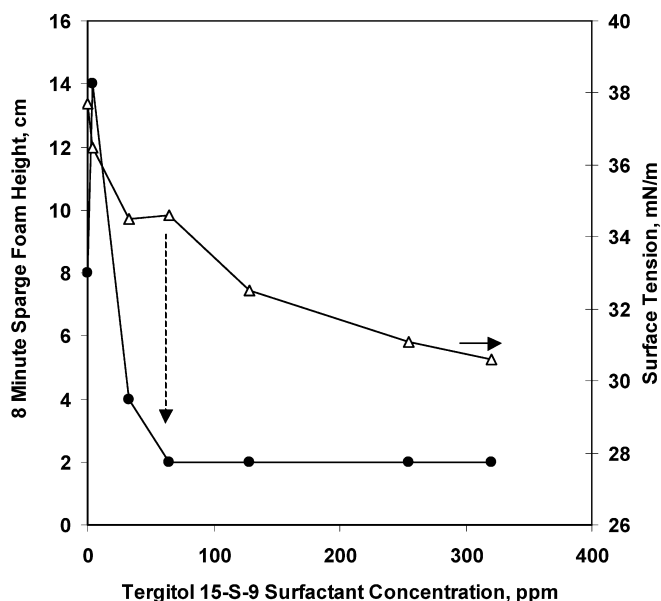


Fig. 7 Sparge test (8-min) foam heights of potato liquor containing 50 ppm of silicone antifoam emulsion and varying in Tergitol 15-S-9 surfactant concentration (*black circles*) Surface tension of potato liquor with added Tergitol 15-S-9 surfactant is also shown (*white triangles*). *Dashed arrow* highlights the correlation of the surface tension inflection with SCAFC

are given, with higher values corresponding with greater water solubility.

Figure 8 explores the relationship between surface pressure and antifoam performance. Performance is expressed as the relative reduction in 8-min foam height, ΔF_{rel} , to allow easier comparison between the different surfactants at various concentrations. The data generally

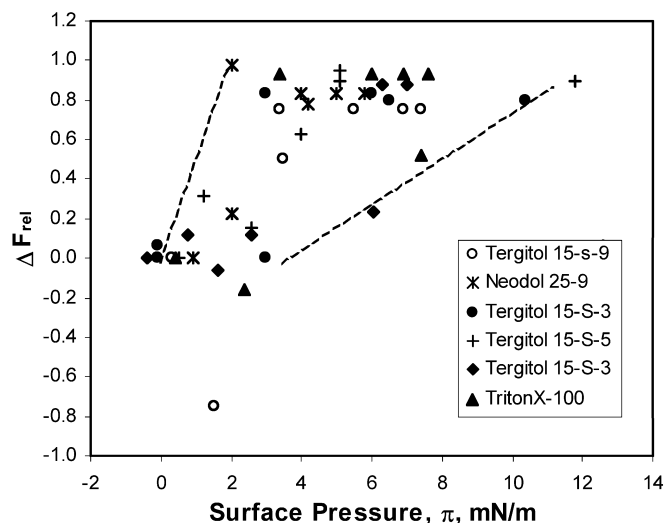


Fig. 8 Surface pressure and relative foam height reduction, ΔF_{rel} , for the ethoxylated surfactants tested in potato liquor sparge tests with silicone antifoam. *Dashed lines* indicate the region of clustering of data points

fall between the ranges suggested by the dotted lines, but there is no easily discernable correlation between surface pressure and antifoam performance.

The surfactant concentration at which there is an inflection-point in the surface tension curve coincides with the SCAFC for five of the eight surfactants tested (highlighted in Table 1). Those not coinciding well show a break at a somewhat higher surfactant concentration. Surfactant adsorption onto components present in the potato liquor decreases the surfactant adsorption at the water surface. The correlation with antifoam performance indicates that surfactant saturation of those components must occur before the surfactant can destabilize the foam. It is not clear from these data whether the components are present in bulk solution or are adsorbed at the water surface.

The adsorption of Tergitol 15-S-7 surfactant onto components in potato liquor was elucidated by comparing surface tension isotherms in water, potato liquor (at 9.1 g solids/l), and liquor diluted with water to give 1.0 g and 5.1 g solids/l. Figure 9 shows rather typical surface tension behavior for Tergitol 15-S-7 in pure water. Surface tension decreases with surfactant concentration, exhibiting a change in slope near the critical micelle concentration (CMC) reported to be 39 ppm [26]. Tergitol 15-S-7 saturation of the water surface is reported to provide a surface tension of 28 mN/m (dashed line). As is often observed with impure commercial grade surfactants, the surface tension dips below the expected minimum at a concentration slightly greater than the CMC.

The surface tension of the potato liquor solutions prior to the addition of surfactant were 48, 42, and 38 mN/m, decreasing with the concentration of solids and were markedly reduced relative to pure water (72 mN/m), due to the presence of surface-active

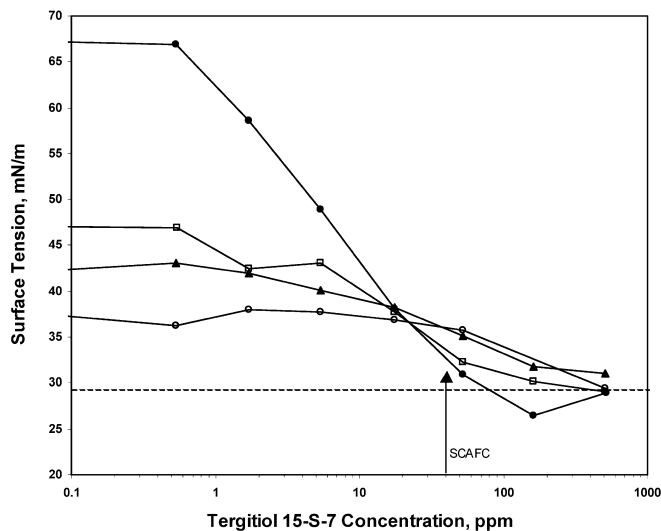


Fig. 9 Surface tension isotherm as Tergitol 15-S-7 concentration is varied in pure water (*black circles*) and in potato liquor diluted to a solids content of 1.0 g/l (*white squares*), 5.1 g/l (*black triangles*), and full-strength potato liquor at 9.1 g/l (*white circles*). Arrow indicates the SCAFC for full-strength potato liquor and *dashed line* indicates the surface tension expected for a surfactant-saturated water surface

materials in the potato liquor. The addition of surfactant to the potato liquor solutions further reduces surface tension, indicating the formation of a mixed surface layer containing potato liquor components and surfactant. At a surfactant concentration of about 500 ppm, the surface tension for all three samples approaches 28 mN/m, suggesting the formation of a surface layer predominately composed of surfactant and lacking potato liquor components. The arrow marks the SCAFC of the full-strength potato liquor. At this concentration, the surface tension increases with the potato liquor solids level and is consistent with surfactant adsorption onto the potato liquor components. This surfactant concentration is considerably below that needed to saturate the surface with surfactant and consequently, at the SCAFC, all of the potato liquor dilutions possess a mixed surface layer. Apparently, the enhanced antifoam performance at the SCAFC does not require the surface layer to be completely free of potato liquor components.

Foam control enhancement varies with surfactant structure. The Tergitol surfactant series is based on the same secondary alcohol but varies in the average number of ethylene oxide units per molecule, i.e. having three, five, seven, or nine. Figure 10 shows that the SCAFC decreases with the degree of ethoxylation. The CMC for these surfactants in pure water [26] shows the expected increase with ethoxylation and is opposite to the trend for SCAFC.

Surfactant hydrophilicity is generally expressed as the HLB [27], with higher values indicating greater water solubility. As shown in Fig. 11, the SCAFC decreases with surfactant HLB for the various kinds of ethoxylated surfactants but does not hold for sodium oleate or for glycerol oleate.

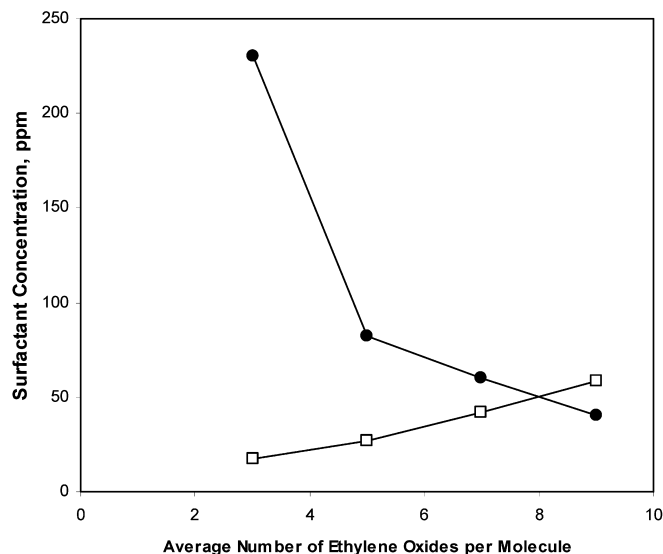


Fig. 10 Variation in the SCAFC (*black circles*) and critical micelle concentration (*white squares*) with average number of ethoxylates per molecule in the Tergitol series

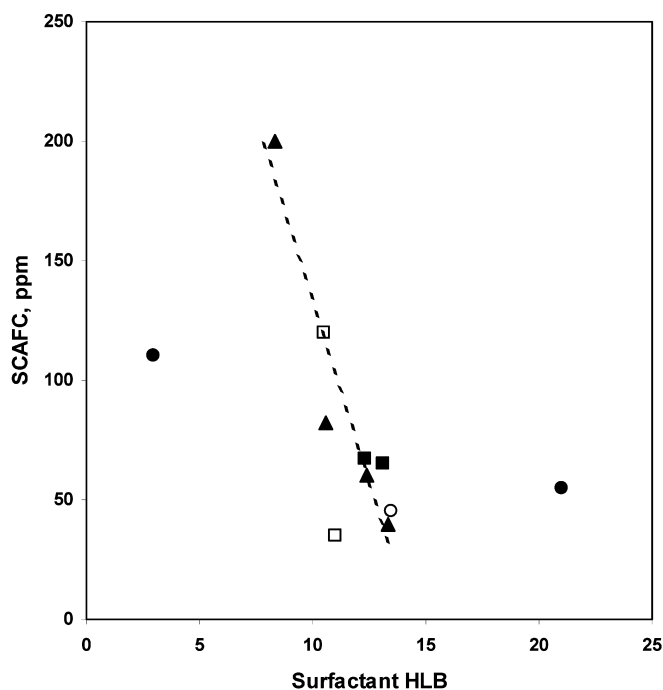


Fig. 11 SCAFC and surfactant hydrophilic-lipophilic balance (HLB) for: linear alcohol ethoxylates (*black squares*), ethoxylated sorbitan fatty acid esters (*white squares*), secondary alcohol ethoxylates (*black triangles*), sodium oleate and glycerol monooleate (*black circles*), and alkylphenol ethoxylate (*white circles*), with a linear regression fit ($R^2=0.70$) through the ethoxylated surfactants (*dotted line*), excluding the sodium oleate and glycerol monooleate

Discussion

Optical microscopy and laser interferometry of potato liquor bubble films establish the important role of par-

ticles derived from biological origins, such as starch particles, in bubble film stabilization. These particles are observed to be immobile in the film and act as “props” that maintain film thickness against the gravitational and capillary forces that drain bubble films. Similar behavior is observed in the stabilization of ovalbumin foams by hydrophobic polystyrene particles [12].

The addition of surfactants to potato liquor improves the extent and the longevity of foam control by a silicone antifoam, with a concentration dependence based on the structure of the surfactant. The surfactant SCAFC is a measure of its mass efficiency, which improves with the degree of ethoxylation and HLB of ethoxylated surfactants. This effect must be a balance between the increased surfactant solubility and a decreased tendency to adsorption. As the degree of ethoxylation increases, the hydrophilic cross-sectional area increases [20], possibly enabling each molecule to “cover” more hydrophobic area on the potato liquor components. Apparently, within a fairly broad range of nonionic surfactant structures, the area of coverage is more important to efficient enhancement of antifoaming.

Surfactant adsorption onto the potato liquor components present in the bulk and at the water surface correlates with the SCAFC and ultimately with a modification of the water surface layer. Two models were proposed to describe the interaction between surfactant and surface-active potato liquor components. There is no surface pressure that correlates with antifoaming performance enhancement and this suggests that a reorganization of the surface layer is not sufficient to promote antifoaming. More likely, surfactant-driven desorption of potato liquor components from the surface is tied to enhanced antifoaming performance. The inflection-point noted in some of the surface tension curves correlates with the SCAFC and marks a change in the adsorption of surfactant at the water surface that is meaningful to antifoaming. These changes are best attributed to the completion of surfactant adsorption onto components present in the bulk potato liquor and the beginning of a displacement of surface-adsorbed potato liquor components. At the SCAFC, desorption of potato liquor components from the surface layer is not complete.

At the surfactant concentration just above the saturation of the bulk potato liquor, surfactant-enhancement of silicone antifoam performance can be summarized as: (1) surface-active components in the potato liquor are present at the water surface and in the bubble film, with hydrophobic regions exposed at the water surface, (2) surfactant adsorbs onto these components at their hydrophobic regions, with the surfactant hydrophilic heads directed towards the solution, (3) at a concentration determined by the surfactant structure, a sufficient coverage of the hydrophobic region occurs, allowing the component to desorb into the underlying solution, (4) once a sufficient amount of a specific type of surface-active potato liquor components is desorbed from the surface, the bubble surface begins

to look more like a surfactant-based foam than a protein foam, and (5) silicone antifoam becomes effective and can match the rate of bubble-rupture to the rate of bubble production. One possible explanation for this rate enhancement is the removal of the steric barriers which prevented antifoam entering.

References

1. Benjamins J, Lucassen-Reynders EH (1998) Surface dilatational rheology of proteins adsorbed at air/water and oil/water interfaces. In: Mobius M, Miller R (eds) *Proteins at liquid interfaces*. Elsevier, New York, p. 341
2. Chen J, Dickinson E (1995) Surface shear viscosity and protein-surfactant interactions in mixed protein films adsorbed at the oil-water interface. *Food Hydrocolloids* 9:35-42
3. Dalgleish DG (1996) Food emulsions. In: Sjoblom J (ed) *Emulsions and emulsion stability*. (Surfactant science series, vol 61) Dekker, New York, pp 287-325
4. Denkov ND, Cooper P, Martin J-Y (1999) Mechanisms of action of mixed solid-liquid antifoams. 1. Dynamics of foam film rupture. *Langmuir* 15:8514
5. Dickinson E (1992) Proteins in solution and at interfaces. In: Goddard ED, Ananthapadmanabhan KP (eds) *Interactions of surfactants with polymers and proteins*. CRC Press, Boca Raton, p. 317
6. Garrett PR (1993) The mode of action of antifoams. In: Garrett PR (ed) *Defoaming theory and industrial applications*. (Surfactant science series, vol 45) Dekker, New York, pp 1-117
7. Graham DE, Phillips MC (1979) Proteins at liquid interfaces. III. Molecular structures of adsorbed films. *J Colloid Interface Sci* 70:427-439
8. Griffin WC (1979). Emulsions. In: Kirk-Othmer Encyclopedia of chemical technology, vol 8, 3rd edn. Wiley, New York, pp 900-930
9. Hall MJ, Dickinson SD, Pritchard R, Evans JI (1973) Foams and foam control in fermentation processes. *Prog Ind Microbiol* 12:171
10. Jha BK, Christiano SP, Shah DO (2000) Silicone antifoam performance: correlation with spreading and surfactant monolayer packing. *Langmuir* 26:9948
11. Koch V, Ruffer H-M, Shugerl K, Innertsberger E, Menzel H, Weis J (1995) Effect of antifoam agents on the medium and microbial cell properties and process performance in small and large reactors. *Process Biochem* 30:435
12. Kumagai H, Trikata Y, Yoshimura H, Katao M, Yano T (1991) *Agric Biol Chem* 55:1823
13. Lobo LA, Wasan DT (1993) Mechanisms of aqueous foam stability in the presence of emulsified non-aqueous-phase liquids: structure and stability of the pseudoemulsion film. *Langmuir* 9:1668-1677
14. Mackie A, Gunning PA, Mackie AR, Kirby AR, Morris VJ (2001) Scanning near field optical microscopy of phase separated regions in a mixed interfacial protein (BSA)-surfactant (Tween 20) film. *Langmuir* 17:2013
15. McCutcheon's emulsifiers and detergents, North American edn., vol 1 (2000) MC Publishing Company, Glen Rock, N.J.
16. Narsimhan G (1996) Foam formation and stabilization. *Curr Opin Colloid Interface Sci* 1:759-763
17. Nobel I (1994) *Conf Adv Biochem Eng* 2:17
18. Petkov JT, Gurkov TD (2000) Dilatational and shear elasticity of gel-like protein layers on air/water interface. *Langmuir* 16:3703
19. Prins A, Riet K van't (1987) Proteins and surface effects in fermentation: foam, antifoam, and mass transfer. *Trends Biotechnol* 5:296
20. Rosen MJ (1994) *Surfactants and interfacial phenomena*, 2nd edn. Wiley, New York

21. Ross S (1967) Mechanisms of foam stabilization and anti-foaming action. *Chem Eng Process* 6:41
22. Roth S, Murray BS, Dickinson E (2000) Interfacial shear rheology of aged and heat-treated β -lactoglobulin films: displacement by nonionic surfactant. *J Agric Food Chem* 48:1491–1497
23. Snow SA, Pernisz UC, Nugent BM, Stevens RE, Braun R, Naire S (2001) Modeling the stabilizing behavior of silicone surfactants during the processing of polyurethane foam; the use of thin liquid films. In: Kempner D, Fritch KC (eds) *Advances in urethane science and technology*. Rapra Technology Ltd, Shawbury, pp 213–260
24. Stanbury PF, Wistaker A, Hall SJ (1995) *Principles of fermentation technology*, 2nd edn. Butterworth–Heinemann, New York
25. Szarka L, Magyar K (1969) The foams of fermentation broths I. Some parameters of the foaming of fermentation media. *Biotechnol Bioeng* 11:701
26. Union Carbide (1989) Tergitol product information guides [F-49980-ICD (11/89-5M), F-49979-ICD (8/89-5M), F-49978-ICD, (8/89-5M), F-49977-ICD, (8/89-5M)]. Union carbide chemicals and plastics company, New York
27. Van Gelder WMJ, Krechting CF (1973) Rapid method of estimating the content of coagulable protein in potato tubers. *Found Agric Plant Breed* 16:311–314
28. Wang G, Pelton R, Hrymak A, Shawafaty N, Heng YM (1999) On the role of hydrophobic particles and surfactants in de-foaming. *Langmuir* 15:2202
29. Wasan DT, Koczo K, Nikolov AD (1994) Mechanisms of aqueous foam stability and antifoaming action with and without oil, a thin-film approach. In: Schramm LL (ed) *Foams: fundamentals and applications in the petroleum industry*. (ACS symposium series, vol 242) American Chemical Society, Washington, D.C., pp 47–114
30. Wasan DT, Christiano SP (1997) Foams and antifoams: a thin film approach. In: Birdi KS (ed) *Handbook of surface and colloid chemistry*. CRC Press, Boca Raton, pp 179–215